Supporting Information

Boron Carbonitride with Tunable B/N Lewis Acid/Base Sites for Enhanced Electrocatalytic Overall Water Splitting

Dong Shi,‡, Bin Chang,‡ Zizheng Ai, Hehe Jiang, Fuzhou Chen, Yongliang Shao, Jianxing Shen, Yongzhong Wu and Xiaopeng Hao**

E-mail: *wuyz@sdu.edu.cn*; *xphao@sdu.edu.cn*

‡ These authors contributed equally to this work.

This file includes:

S1. Materials

Boric acid and urea were purchased from Sinopharm Chemical Reagent Co. Ltd (Shanghai). PEG-2000 was purchased from Aladdin Reagent Co., Ltd. All the reagents were of A. R. grade and used as received without further purification.

S2. Experimental Section

2.1 Density functional theory (DFT) calculations

All calculations were carried out by using the projector augmented wave method in the framework of the density functional theory (DFT),[1] as implemented in the Vienna *ab*-initio Simulation Package (VASP). The generalized gradient approximation (GGA) and Perdew–Burke–Ernzerhof (PBE) exchange functional[1] was used. The plane-wave energy cutoff was set to 520 eV, and the Monkhorst–Pack method[2] was employed for the Brillouin zone sampling. The convergence criterions of energy and force calculations were set to 10^{-5} eV/atom and 0.01 eV $Å^{-1}$, respectively. To explore the interactions between the H_2O and OH* molecule and BCN monolayers, the adsorption energies of the H_2O and OH* molecule on the BCN surfaces were calculated. The B-BCN and N-BCN monolayer were built by replacing part of C atoms in graphene with B and N atoms by the composition of B: N: C = 2: 1: 1 and 1: 2: 1, respectively, as shown in **Figure S1** (**Supporting Information**). A vacuum region of 15 Å is applied to avoid interactions between the neighboring configurations. DFT-D2 method was used to account for the van der Waals interactions between the molecule and BCN surface. Here, the adsorption energies (E_a) were calculated by the energy difference of the system after and before adsorption[3]: E_a= E(H_2O or OH*-BCN)–E(H_2O or OH*)–E(BCN), where E(H_2O or OH*-BCN), E(H_2O or OH*), and E(BCN) represent the DFT energies of the H_2O or OH*molecule adsorbed BCN surface, the energy of an isolated H_2O or OH* molecule and the energy of the clean BCN surface.

2.2 Synthesis of B-BCN

In a typical synthesis process of B-BCN, 1.0 g boric acid, 10.0 g urea, and 1.5 g PEG-2000 were dissolved in 35 mL deionized water under stirring for 5-10 minutes. Next, the solution was transferred to a porcelain boat with carbon paper on the bottom. Then, the porcelain boat was moved to a heating stage and dried at 100 ℃ for 12 hours. Finally, the fully dried precursor was pyrolysed at 900 ℃ for 6 hours under Ar atmosphere to obtain the target sample which was marked as B-BCN-2. Furthermore, we changed the content of boric acid to 0.15 g and 0.8 g to prepare B-BCN-1 and B-BCN-3 samples.

2.3 Synthesis of N-BCN

In a typical synthesis process of N-BCN, 0.3 g boric acid, 20.0 g urea, and 1.5 g PEG-2000 were dissolved in 35 mL deionized water under stirring for 5-10 minutes. The subsequent operation steps are the same as those during the preparation of B-BCN. Finally, we obtained N-BCN-2 sample. Furthermore, we changed the content of boric acid to 10 g and 20 g to prepare N-BCN-1 and N-BCN-3 samples.

2.4 Materials characterization

Scanning electron microscopy (SEM) images were obtained with a Hitachi S-4800 field-emission scanning electron microscope. High-resolution TEM (HRTEM) images were obtained using a Philips Tecnai 20UTwin microscope at an acceleration voltage of 200 kV. The solution of samples was achieved after 15 min ultrasonic pretreatment. The TEM samples were prepared by dropping the primed solution onto a copper grid with polyvinyl formal support film and dried in air. X-ray diffraction (XRD) patterns of the materials were obtained on a diffractometer (Bruker D8) using a Cu Kα radiation source (λ =0.15418 nm) with a 2θ scan from 10 to 70 with a step size of 0.06. X-ray photoelectron spectroscopy (XPS) measurements of all materials were performed on a Thermo ESCALAB 250 X-ray photoelectron spectrometer using monochromated Al K radiation (1486.8 eV). All of the binding energies were calibrated to the C 1s peak at 284.6 eV of the surface adventitious carbon.

2.5 Electrochemical characterization

Electrochemical measurements were tested in a three-electrode system using an electrochemical workstation (CHI 760D). Ag/AgCl (KCl saturated, $E^0_{Ag/AgCl}$ = 0.2046 V, at 25 ℃) and Pt were used as reference and counter electrodes, respectively. The as-prepared B/N-BCN was used as a working electrode. Polarization curves of hydrogen or oxygen generation were obtained using linear sweep voltammetry (LSV) with a scan rate of 2 mV s^{-1} at 25 ℃ in the aqueous solutions (1.0 M KOH) with constant N_2 (g) continually purging for 30 min prior to the measurements. In all measurements, the Ag/AgCl reference electrode was calibrated with respect to the reversible hydrogen electrode (RHE). The potentials of HER/OER measurement were converted to RHE using the equation given by $E_{RHE} = E_{Ag/AgCl} + 0.0591\ PH + 0.194$, resulting in a shift of +1.0155V vs. RHE in 1.0 M KOH solution (pH~13.9). The long-term stability test was measured using chronopotentiometric measurements. Overall water splitting was performed in a two-electrode system. B-BCN electrode acted as the positive electrode for OER and N-BCN electrode was used as the negative electrode for HER.

S3. Supplementary Figures

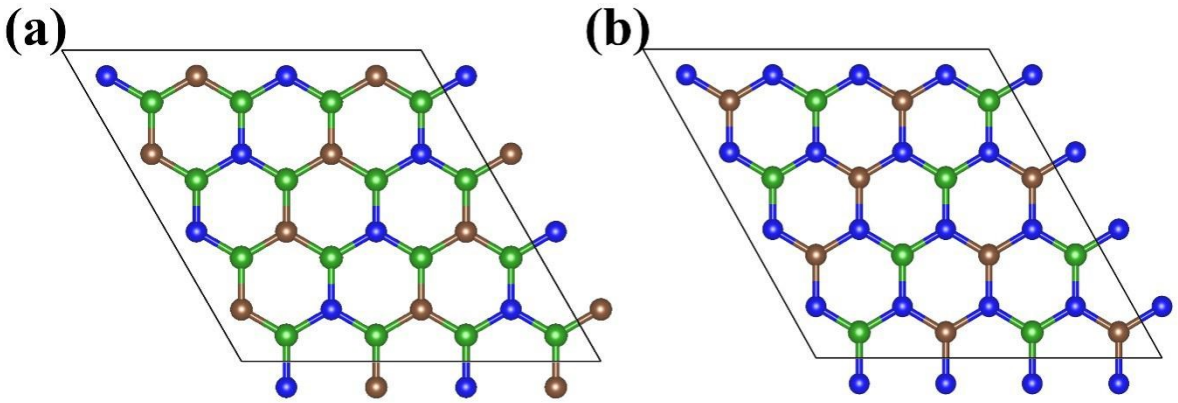

Figure S1. Structure of (a) B-BCN and (b) N-BCN monolayer. The green, blue, and brown balls donate B, N, and C atoms, respectively.

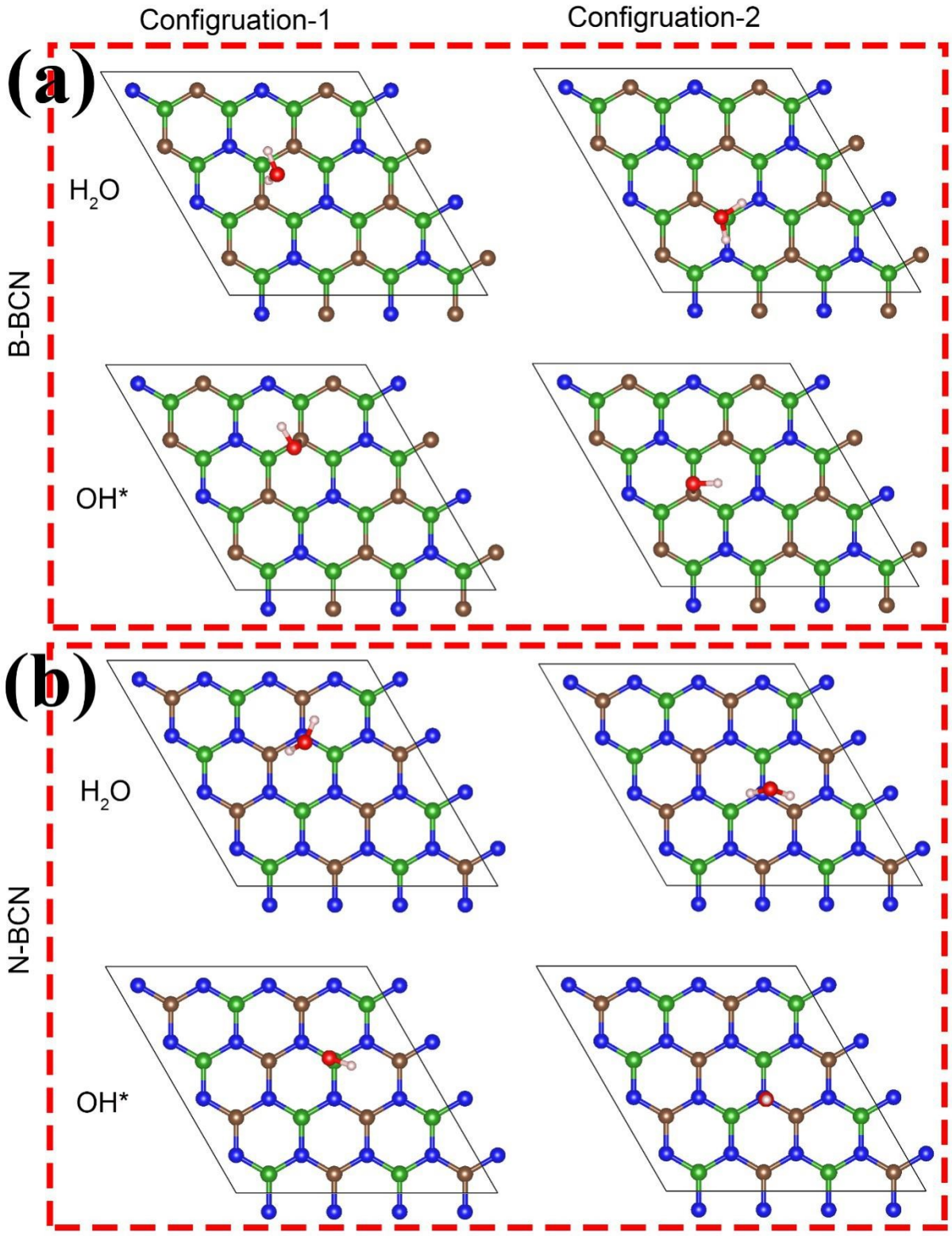

Figure S2. Optimized structures of H_2O and OH* molecule adsorption on the (a) B-BCN and (b) N-BCN monolayer. The green, blue, brown, red, and pink balls donate B, N, C, O and H atoms, respectively.

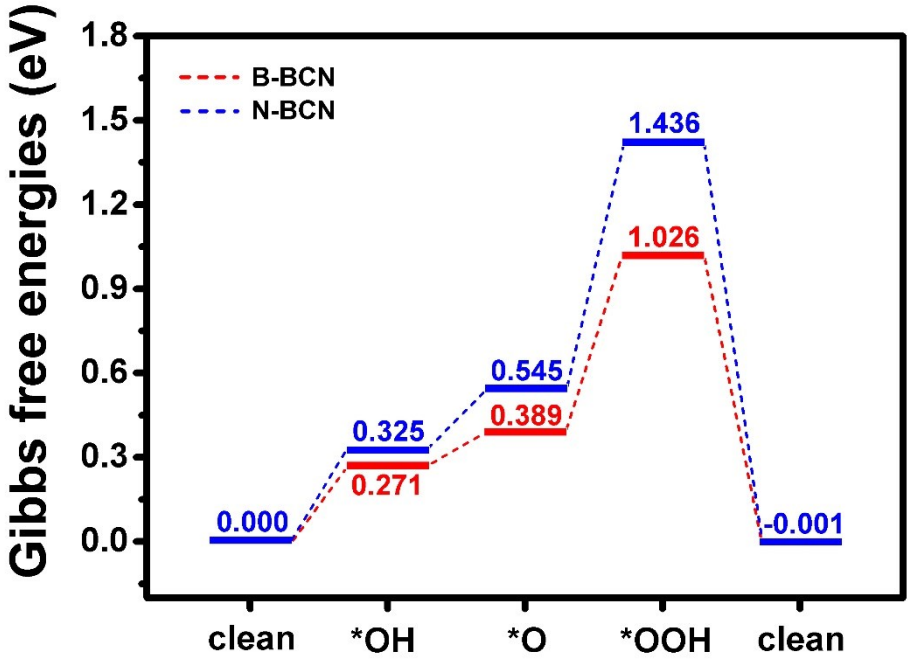

Figure S3. Gibbs free energy profiles of OER reaction on B-BCN and N-BCN monolayer.

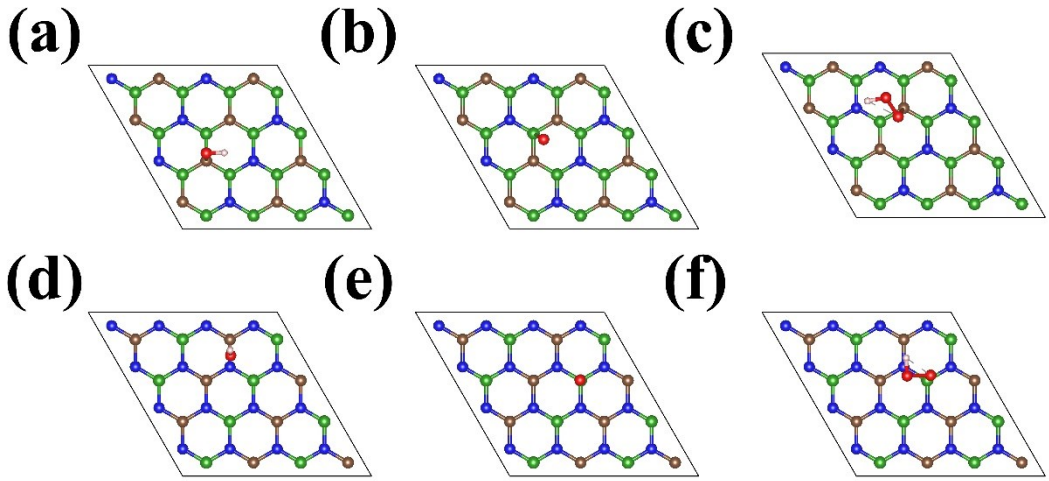

Figure S4. Schematic diagram of adsorption position of different intermediates in each step of OER process: B-BCN structure, (a) *OH, (b) *O, (c) *OOH; N-BCN structure, (d) *OH, (e) *O, (f) *OOH.

The free energy changes of each step of oxygen evolution reaction on B-BCN and N-BCN surfaces are obtained by DFT calculation method. The OER occur via the following steps[4]:

$$4OH^- + * \rightarrow *OH + 3OH^- + e^- \quad (1)$$

$$*OH + 3OH^- + e^- \rightarrow *O + H_2O + 2OH^- + 2e^- \quad (2)$$

$$*O + H_2O + 2\,OH^- + 2e^- \rightarrow *OOH + H_2O + OH^- + 3e^- \quad (3)$$

$$*OOH + H_2O + OH^- + 3e^- \rightarrow O_2 + 2H_2O + 4e- + * \quad (4)$$

The calculated Gibbs free energy profiles of OER reaction on B-BCN and N-BCN monolayer following the suggested reaction pathways are presented in **Figure S3** (**Supporting Information**). And the schematic diagram of adsorption position of different intermediates in each step of OER process is shown in **Figure S4** (**Supporting Information**). One important parameter that can be used to evaluate the catalytic activity is the limiting reaction barrier, which is determined from the free energy of the rate-determining step (RDS)[4]. For both N-BCN and B-BCN, the RDS is the oxidation of O* to OOH* with limiting barrier as large as 0.891 and 0.637 eV. And the overpotentials of B-BCN and N-BCN are 0.637 and 0.891 eV, respectively. It can be clearly observed from the figure that BCN exhibits the lowest energy barrier and the lowest theoretical overpotential, which is consistent with our experimental results. Also, the thermodynamic onset potential of OER process[5] is extracted from **Table S4** (**Supporting Information**): $U_{onset}=U_{*OOH}-U_{*O}$= 2.17 eV-0.96 eV=1.21 eV.

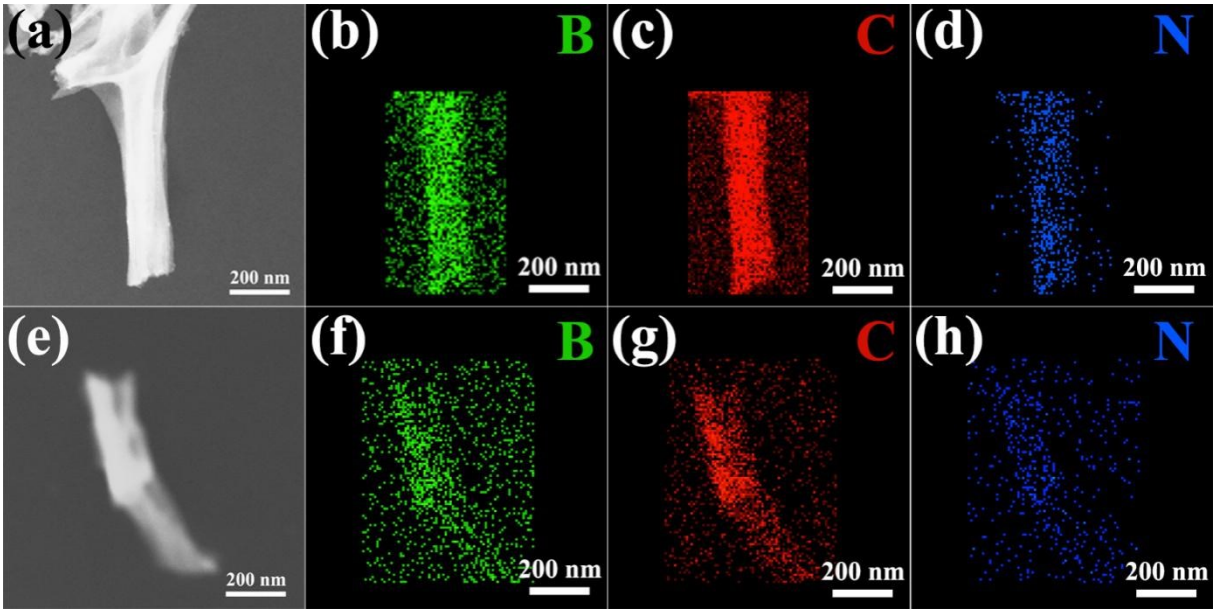

Figure S5. (a) TEM image of B-BCN. (b)-(d) TEM mapping of B-BCN. (e) TEM image of N-BCN. (f)-(h) TEM mapping of N-BCN.

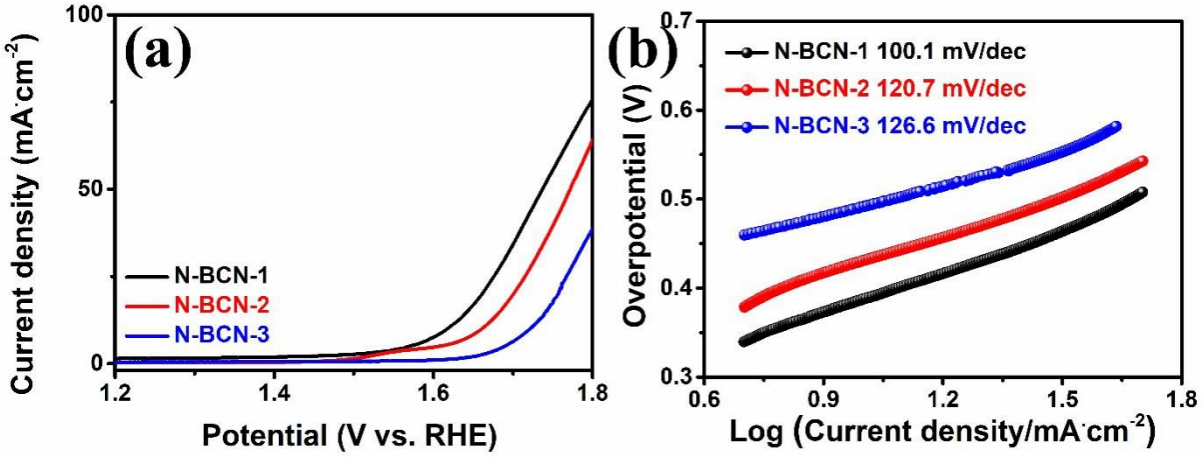

Figure S6. (a) OER polarization curves of N-BCN samples. (b) Tafel slope curves corresponding to OER polarization curves.

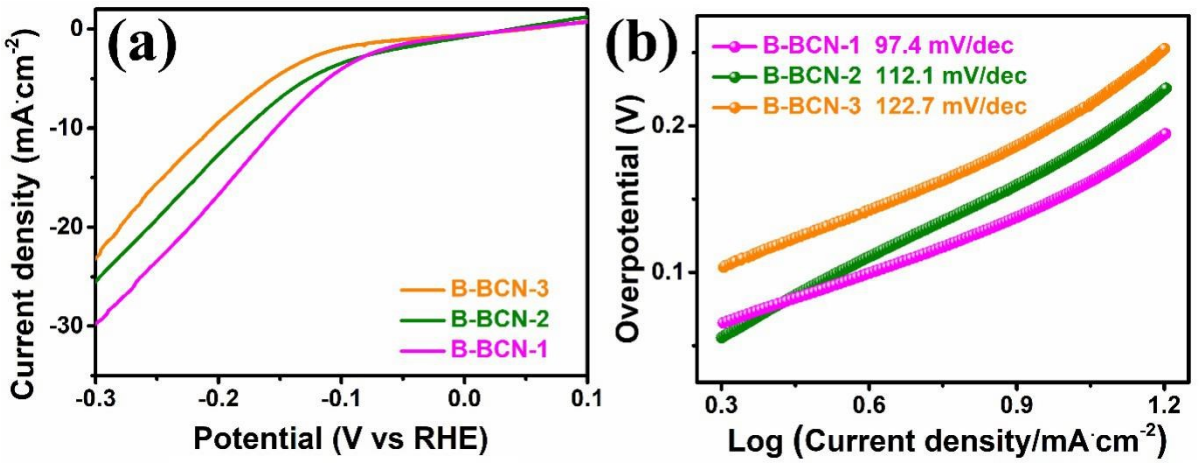

Figure S7. (a) HER polarization curves of B-BCN samples. (b) Tafel slope curves corresponding to HER polarization curves.

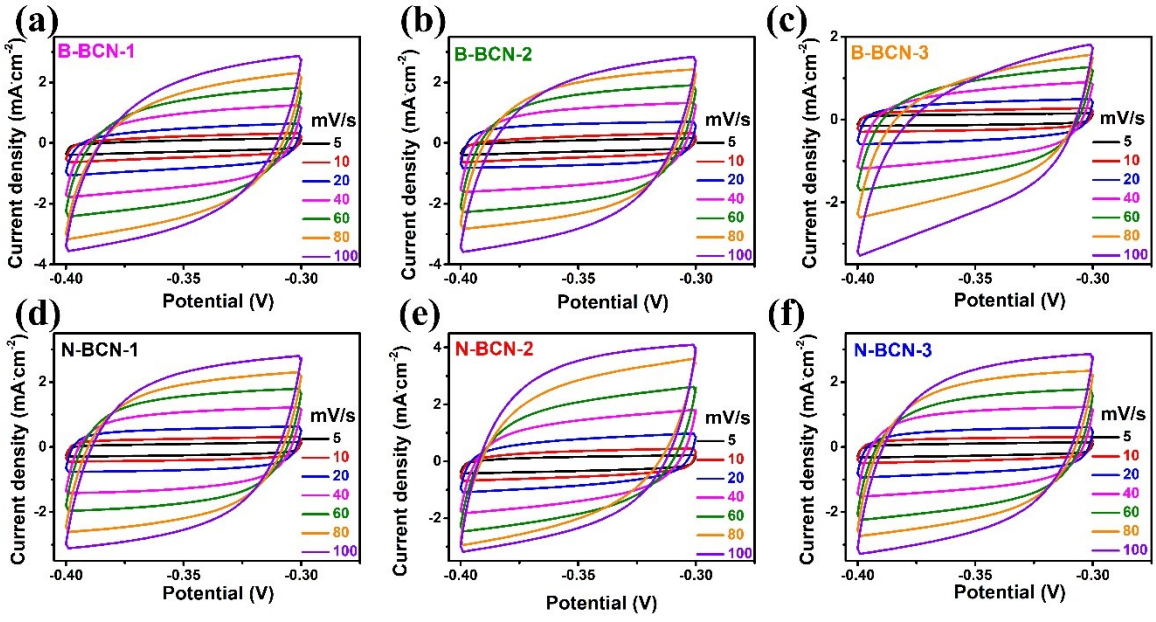

Figure S8. Electrochemical cyclic voltammetry curves at different potential scanning rates for B-BCN (a)-(c) and N-BCN (d)-(f).

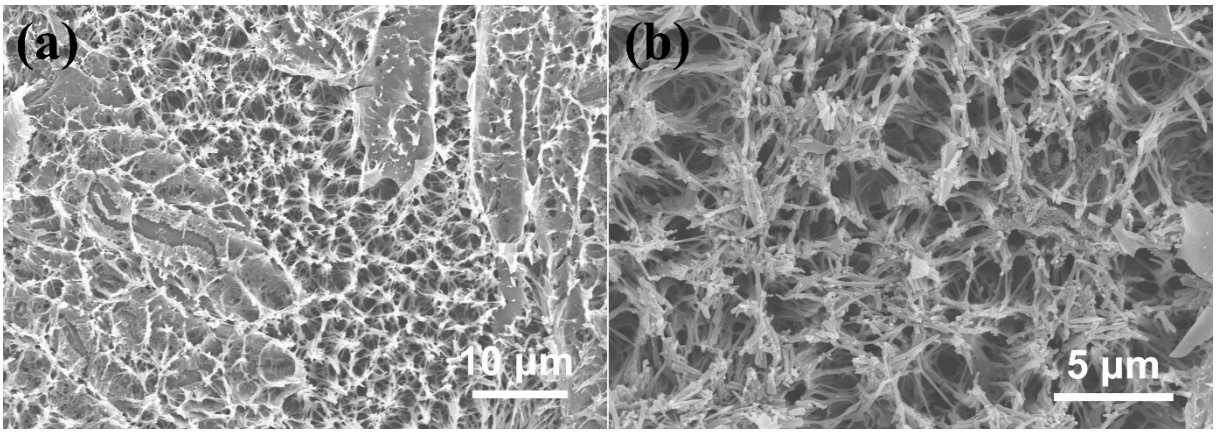

Figure S9. (a) SEM image of B-BCN after stability tests. (b) SEM image of N-BCN after stability tests.

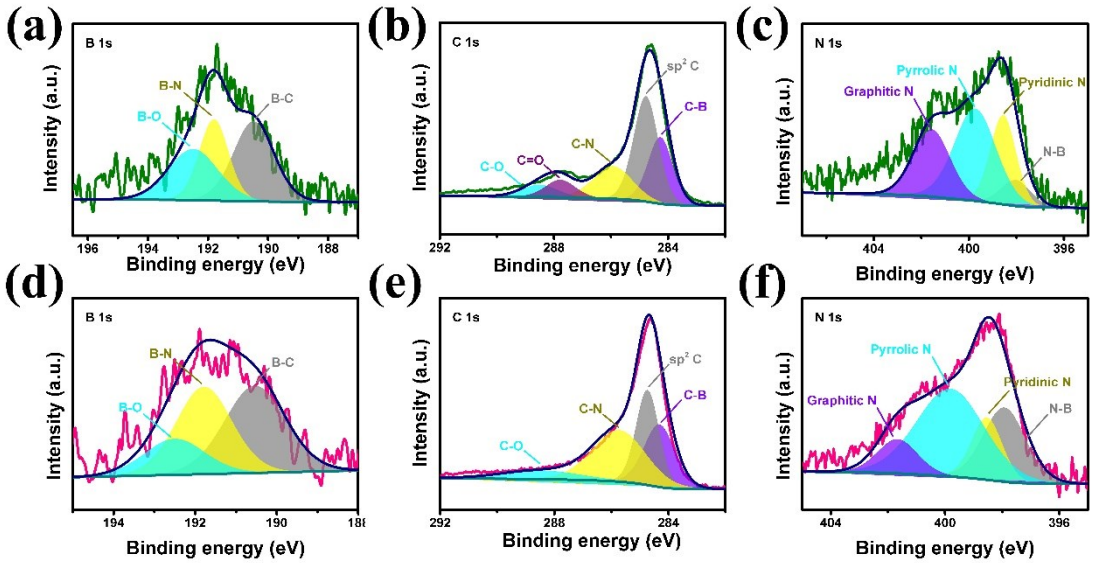

Figure S10. High-resolution XPS spectra after durability tests of B-BCN samples: (a) B 1s, (b) C 1s, (c) N 1s; N-BCN: (d) B 1s, (e) C 1s, (f) N 1s.

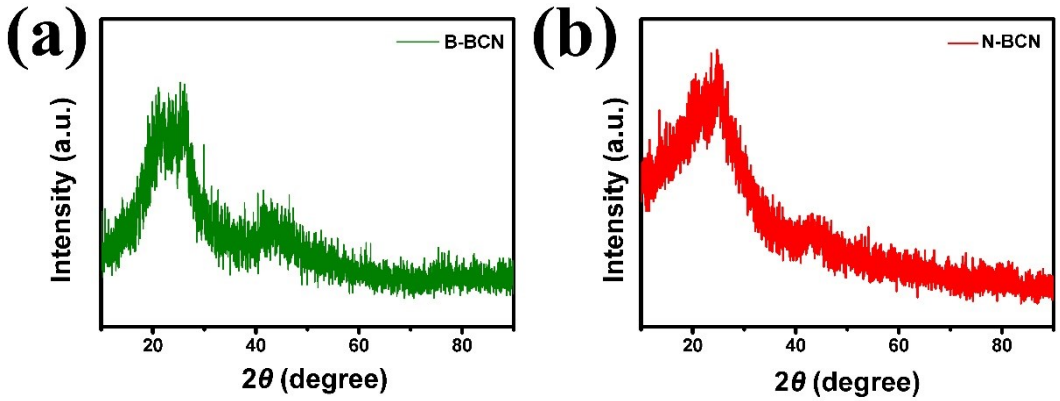

Figure S11. XRD patterns of B-BCN and N-BCN after durability tests.

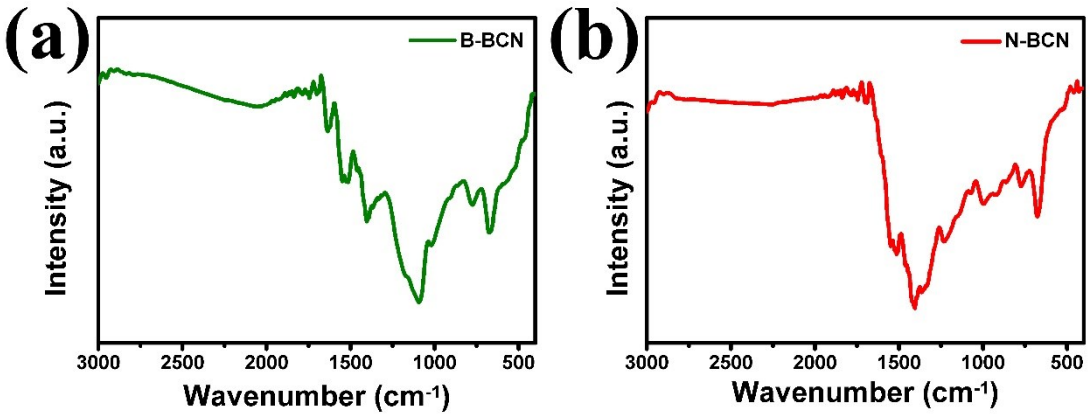

Figure S12. FTIR spectra of B-BCN and N-BCN after durability tests.

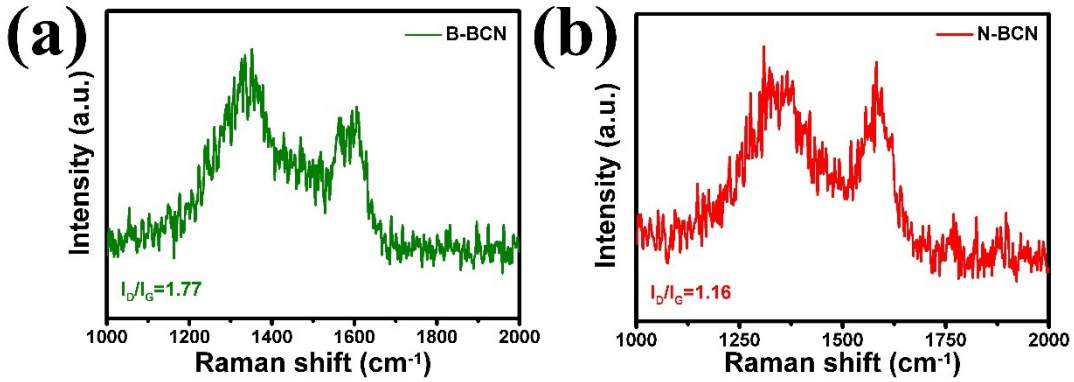

Figure S13. Raman spectra of B-BCN and N-BCN after durability tests.

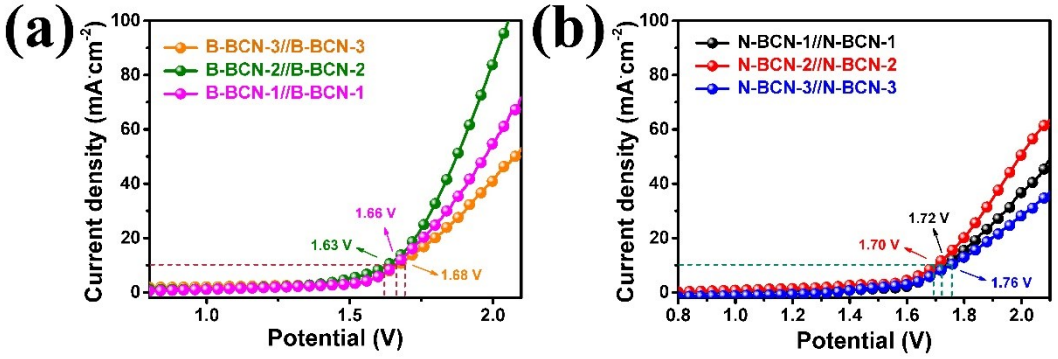

Figure S14. The polarization curves of BCN system with different B/N ratios.

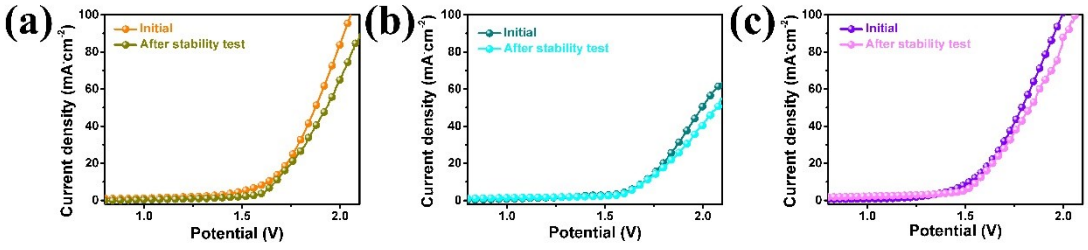

Figure S15. The polarization curves before and after electrochemical stability tests of (a) B-BCN//B-BCN, (b) N-BCN//N-BCN, and (c) B-BCN//N-BCN systems.

Table S1. Elemental analysis of the as-obtained BCN materials.

Element Atomic %	Sample					
	B-BCN-1	B-BCN-2	B-BCN-3	N-BCN-1	N-BCN-2	N-BCN-3
B	16.46	13.87	16.98	9.82	4.26	5.12
C	69.70	71.87	78.40	67.24	76.03	70.31
N	11.02	6.32	4.62	11.62	11.85	16.93
O	2.82	7.94	-	11.32	7.86	7.64
B:N	1.5:1	2.2:1	3.7:1	1:1.2	1:2.8	1:3.3

Table S2. Electrocatalytic HER performance of currently reported materials for comparison.

Samples	Overpotential (η_{10}, mV)	Tafel slope (mV dec^{-1})
Pt/C[6]	~70	~60
MoS_2@C[7]	155	99
N, F-doped graphene[8]	330	109
WC/graphene[9]	225	108
N, S-doped CNT[10]	~450	133
N, P-doped graphene[11]	~480	145
N-BCN (This work)	**142.7**	**61.3**

Table S3. Electrocatalytic OER performance of reported materials currently for comparison.

Samples	Overpotential (η_{10}, mV)	Tafel slope (mV dec^{-1})
IrO_2[12]	~320	49
NiFe LDH/3D carbon[13]	380	77.9
NiFeMo LDH[14]	280	75
β-$Co(OH)_2$/RGO[15]	320	66
α-$Co(OH)_2$/CNT[16]	254	84
ZnCo LDH[17]	450	101

B-BCN (This work)	**158.9**	**65.2**

Table S4. Gibbs free energy for OER process.

Step	**U (potential, V)=0**				
	clean	*OH	*O	*OOH	clean
Gibbs free energy (eV)	0.00	0.65	0.96	2.17	1.61

S4. Supplementary References

1 W. Kohn and L. J. Sham, *Phys. Rev.*, 1965, **140**, 1133.

2 M. H and P. J, *Phys. Rev. B*, 1976, **12**, 5188.

3 X. Lv, Z. Xu, J. Li, J. Chen and Q. Liu, *Appl. Surf. Sci.*, 2016, **376**, 97.

4 H. Fei, J. Dong, Y. Feng, C.S. Allen, C. Wan, B. Volosskiy, M. Li, Z. Zhao, Y. Wang, H. Sun, P. An, W. Chen, Z. Guo, C. Lee, D. Chen, I. Shakir, M. Liu, T. Hu, Y. Li, A.I. Kirkland, X. Duan and Y. Huang, *Nat. Catal.*, 2018, **1**, 63-72.

5 D. Alfonso, D. Tafen and D. Kauffmann, *Catalysts*, 2018, **8**, 424.

6 J. Chen, Y. Yang, J. Su, P. Jiang, G. Xia and Q. Chen, *ACS Appl. Mater. Inter.*, 2017, **9**, 3596-3601.

7 Q. Xu, Y. Liu, H. Jiang, Y. Hu, H. Liu and C. Li, *Adv. Energy Mater.*, 2019, **9**, 1802553.

8 M.A.R. Anjum, H.Y. Jeong, M.H. Lee, H.S. Shin and J.S. Lee, *Adv. Mater.*, 2018, **30**, 1707105.

9 M. Zeng, Y. Chen, J. Li, H. Xue, R.G. Mendes, J. Liu, T. Zhang, M.H. Rümmeli and L. Fu, *Nano Energy*, 2017, **33**, 356-362.

10 K. Qu, Y. Zheng, Y. Jiao, X. Zhang, S. Dai and S. Qiao, *Adv. Energy Mater.*, 2017, **7**, 1602068.

11 Y. Zheng, Y. Jiao, L.H. Li, T. Xing, Y. Chen, M. Jaroniec and S.Z. Qiao, *ACS Nano*, 2014, **8**, 5290-5296.

12 F. Song and X. Hu, *J. Am. Chem. Soc.*, 2014, **136**, 16481-16484.

13 Y. Li, M. Zhao, Y. Zhao, L. Song and Z. Zhang, *Part. Part. Syst. Char.*, 2016, **33**, 158-166.

14 Y. Jin, S. Huang, X. Yue, H. Du and P.K. Shen, *ACS Catal.*, 2018, **8**, 2359-2363.

15 L. Wang, J. Zhang, W. Jiang, H. Zhao and H. Liu, *Appl. Surf. Sci.*, 2018, **433**, 88-93.

16 J. Wu, J. Subramaniam, Y. Liu, D. Geng and X. Meng, *J. Alloy Compd.*, 2018, **731**, 766-773.

17 C. Qiao, Y. Zhang, Y. Zhu, C. Cao, X. Bao and J. Xu, *J. Mater. Chem. A*, 2015, **3**, 6878-6883.